Hybridization of Short Complementary PNAs to G-Quadruplex Forming Oligonucleotides: an Electrospray Mass Spectrometry Study

Jussara Amato,[1] Giorgia Oliviero,[1] Edwin De Pauw,[2] Valérie Gabelica[2,*]

[1] Dipartimento di Chimica delle Sostanze Naturali, Facoltà di Scienze Biotecnologiche, Università di Napoli Federico II, Italy

[2] Physical Chemistry and Mass Spectrometry Laboratory, Department of Chemistry, University of Liège, Belgium

Corresponding author: v.gabelica@ulg.ac.be

Abstract

We investigated the interaction of the short PNA strand [acccca]-PNA with oligodeoxynucleotides containing one, two, or four tracts of TGGGGT units. Electrospray ionization mass spectrometry allowed exploring the wide variety of complex stoichiometries that were found to coexist in solution. In water, the PNA strand forms short heteroduplexes with the complementary DNA sequences, but higher-order structures are also found, with PNA_{2n}•DNA_n triplex units, culminating in precipitation at very low ionic strength. In the presence of ammonium acetate, there is a competition between PNA•DNA heteroduplex formation and DNA G-quadruplex formation. Heteroduplex formation is favored when the PNA + DNA mixture in ammonium acetate is heated and cooled at room temperature, but not if the PNA is added at room temperature to the pre-formed G-quadruplex. We also found that the short [acccca]-PNA strand binds to G-quadruplexes.

Introduction

Guanine Rich Oligonucleotides (GROs) are known to fold into orderly secondary structures stabilized by guanine quartets, which are called G-quadruplexes. Cations (typically Na^+ or K^+) located between quartets participate in cation-dipole interactions with guanines, thereby reducing the repulsion of the central oxygen atoms, enhancing hydrogen bond strength, and stabilizing G-quartets stacking.[1-4] G-rich sequences with the potential to form quadruplex structures are common in genomic DNA, and these have been identified in several biologically important regions, such as the telomeric ends of eukaryotic chromosomes,[5-7] gene promoters,[8-12] or mammalian immunoglobulin heavy chain switch regions.[13,14] Furthermore GROs constitute the scaffold of several aptamers that have the ability to selectively bind to biologically relevant proteins and small molecules.[15-19]

Due to the growing awareness of the biological value of quadruplex structures, great efforts are dedicated in seeking for novel ligands capable of specifically binding to DNA quadruplex-forming oligonucleotides (QFOs). Such ligands could be used as therapeutics agents, diagnostic tools, and molecular probes. The different strategies so far proposed to target DNA quadruplexes make use of: (1) small molecules with large aromatic surfaces that interact with the quadruplex via π-stacking to the guanine tetrads;[20,21] (2) molecules that selectively bind to the grooves of the quadruplex structures;[21,22] and (3) peptide nucleic acids (PNA). PNAs are a class of nuclease-resistant DNA mimics that selectively bind to their complementary DNA targets with higher affinity than the corresponding DNA analogues.[23] Targeting G-quadruplex structures with PNA's can be done using C-rich PNAs that form duplexes with the G-rich strand,[24-27] or G-rich PNAs that are able to form hybrid G-quadruplexes.[26-30]

In this context, we have investigated the interaction between several QFOs, each containing one or more TGGGGT motif, and the short complementary [ac$_4$a]-PNA. QFOs can adopt a variety of folds differing mainly by the number of the DNA strands involved and the relative orientation of the strands into the resulting G-quadruplexes (parallel or antiparallel orientation).[31-33] Since it is known that loop length and sequence plays a key role in determining quadruplex stability and structure,[34-39] we have examined how changes in the loop length (here the number of thymines in the loops) affect G-rich oligonucleotides interaction, both in their folded (quadruplex) and unfolded form. Intermolecular QFOs have been studied, too.

Electrospray mass spectrometry (ESI-MS) was used to evaluate the stoichiometry of complexes. The coupling of an electrospray source to a mass spectrometer was first reported by Fenn and co-workers in 1984,[40-42] In electrospray, the analytes present in solution as ions (for nucleic acids, as anions) are extracted by an electric field applied to the tip of a capillary containing the sample in solution. After the evaporation of the charged droplets, analytes in the form of desolvated ions are transferred into the mass spectrometer. Furthermore, if the evaporation and transfer steps are conducted in soft conditions, intact noncovalently bound DNA structures like duplexes,[43,44] quadruplexes,[39,44-48] and PNA•DNA assemblies[49-52] can be preserved from the solution and detected in the mass spectrometer. Three review articles[53-55] describing various application of mass spectrometry for the study of nucleic acid non-covalent complexes by ESI-MS can be consulted for more references.

Our initial aim was to determine whether a short PNA complementary to only one 4-guanine repeat was capable of unfolding the quadruplex by making several short duplexes like beads on a string. As the present study illustrates, the power of ESI-MS to resolve complex mixtures is crucial for the discovery of novel and sometimes unexpected structures.

Materials and Methods

G-quadruplex sample preparation

The DNA strands were purchased from Eurogentec (Seraing, Belgium) with Oligold™ quality. Ammonium acetate was obtained from a 5 M solution from Fluka (Molecular Biology grade). The procedures described in this paragraph are common to CD, UV and ESI-MS analyses. The lyophilized samples were diluted in water to obtain a 200, 400 or 800 μM stock solutions. The G-quadruplexes were prepared at a concentration of 50 μM (quadruplex concentration), i.e. strand concentration was 50 μM for intramolecular QFOs, 100 μM for bimolecular QFOs, and 200 μM for the tetramolecular QFOs. Quadruplexes (in 10 or 150 mM NH_4OAc) have been prepared heating the 50 μM quadruplex solution at 90 °C for 15 min, followed by fast cooling at 5 °C and storage at the same temperature overnight. DNA solutions in H_2O were also heated at 90 °C for 15 min to disrupt secondary structures, cooled and stored at 5 °C. All DNA samples were analyzed after 16 h at 5 °C. The samples have been diluted just before each experiment to obtain a final quadruplex concentration of 3 μM for CD and UV experiments and 10 μM for ESI-MS analysis.

Preparation of QFO-PNA complexes

The [acccca]-PNA used for DNA hybridization is an unmodified free amine PNA sequence, that has been purchased from PRIMM (Milano, Italy). In 10 and 150 mM ammonium acetate, two different preparation procedures have been tested. (1) At 25 °C: mixing of 40 μM PNA with 10 μM pre-formed G-quadruplex (10 μM is the G-quadruplex concentration), storing for 8 h at 25°C and placing in the fridge at 5 °C overnight. (2) At 90 °C: mixing of 40 μM PNA with 10 μM QFO at 90 °C (the heated QFO was from the pre-formed quadruplex solutions), rapid

cooling to and storing at 25 °C for 8 h, followed by overnight storage at 5 °C. In water, as no G-quadruplex is formed, only the mixing at 25 °C was tested, the oligodeoxynucleotide strand concentration was 10 μM in all cases, and the PNA concentration was set so as to equivalent to the 'TGGGGT' concentration, i.e. 4 equivalents of PNA for TG4T2-intra, TG4T3-intra and TG4T4-intra, 2 equivalents of PNA for TG4T3-bi, and 1 equivalent for TG4T and T4G4T4.

Electrospray mass spectrometry (ESI-MS)

ESI-MS studies were conducted on a Q-TOF Ultima Global (Waters, Manchester, UK). The samples (DNA strand concentration = 10 μM) were infused at 4 μL/min in the electrospray source that was operated in negative ion mode (capillary voltage = -2.2 kV). The source temperature is 80 °C and the nitrogen desolvation gas is 100 °C. The pressure indicated on the source Pirani gauge was 3.0 mbar. For each sample, spectra were recorded using different sets of acceleration voltages: cone voltage was varied from 80 V to 150 V, RF Lens 1 voltage was varied from 50 to 180 V, and collision energy (acceleration voltage before the collision hexapole) was varied from 10 to 20 V. The lowest voltages give the softest source conditions at the chosen source pressure, and are used for example to preserve the ammonium cations inside the G-quadruplexes. However, at low voltages, complexes of higher m/z are not transmitted efficiently through the mass spectrometer, and are therefore not detected efficiently. Therefore, several spectra are recorded at increasing voltages in order to be able to enhance the signal-to-noise ratio of larger complexes. The list of detected species in Tables 2 and 4 includes all species that could be observed, but it must be noted that all of them are not necessarily present simultaneously in a mass scan.

To search the compounds, scans recorded at various voltage settings are summed so that all peaks are displayed simultaneously. The spectra are smoothed (2 × mean, 10 channels), background was subtracted (polynomial order = 50, 1% below curve), and converted to centroid. The compounds were manually searched with the assistance of the MassLynx 4.0 software. Two consecutive peaks that are suspected of pertaining to the same charge distribution are manually picked, and the software searches for further peaks of the charge distribution. If one or more additional peaks are found, the average mass is calculated with its standard deviation.

Circular dichroism

CD spectra were measured on a Jasco J-715 spectropolarimeter equipped by a Peltier Jasco JPT423S. Oligonucleotide solutions (3 μM) were prepared in 150 mM ammonium acetate at pH = 7.0. The samples were heated to 90 °C, annealed by fast cooling at 5 °C and equilibrated one night at that temperature. Spectra were recorded between 220 and 320 nm in 1 mm path length cuvettes. Spectra were averaged over 10 scans, which were recorded at 100 nm/min with a response time of 1 s and a bandwidth of 1 nm. A buffer baseline was subtracted from each spectrum and the spectra were normalized to have zero at 320 nm. A temperature range of 25-90 °C was used to record CD melting profiles both at 295 nm and at 261 nm at a heating rate of 0.5 °C/min.

UV-melting experiments

Oligonucleotides were dissolved in 10 or 150 mM NH_4OAc, pH = 7.0 buffer at a final concentration of 3 μM. Oligonucleotides were annealed by boiling for 15 min, fast cooling to 5 °C and overnight incubation at that temperature. Samples (1.5 mL which filled the cuvette) were placed in quartz cuvettes of 0.5 cm path length. Thermal denaturation was carried out using a

Jasco V-530 UV-visible spectrophotometer equipped with a Jasco ETC-505-T temperature controller. A temperature range of 5-90°C was used to monitor absorbance at 295 nm at a heating rate of 0.5 °C/min. The melting temperatures were calculated as the temperature where the absorbance at 295 nm was halfway between the absorbance of the annealed species and the absorbance of the denatured species.

Results and Discussion

G-quadruplex formation and stability in the absence of PNA

The formation of G-quadruplex structures by the six sequences listed in Table 1 was investigated using circular dichroism (CD), UV-melting monitored at 295 nm, and electrospray mass spectrometry (ESI-MS). CD provides information on the strand orientation in the G-quadruplex (degree of parallel and antiparallel strand conformation), UV-melting provides information on the stability of the G-quadruplex via the melting temperature, and ESI-MS provides information on the stoichiometry of the structures formed (number of strands and number of cations embedded) and on sample heterogeneity.

Table 1: List of studied G-quadruplex forming DNA sequences.

Annotation	**Full DNA sequence**	**Expected G-quadruplex**
TG4T2-intra	dTGGGGTTGGGGTTGGGGTTGGGGT	Intramolecular
TG4T3-intra	dTGGGGTTTGGGGTTTGGGGTTTGGGGT	Intramolecular
TG4T4-intra	dTGGGGTTTTGGGGTTTTGGGGTTTTGGGGT	Intramolecular
TG4T3-bi	dTGGGGTTTGGGGT	Bimolecular
TG4T	dTGGGGT	Tetramolecular
T4G4T4	dTTTTGGGGTTTT	Tetramolecular

Electrospray mass spectrometry (ESI-MS)

When recorded in water, without added ions, the ESI-MS spectra show peaks corresponding to the monomer at different charge states. G-quadruplex formation however requires the presence of cations, and the cation which is both fully compatible at high concentrations with conventional ESI-MS and able to induce G-quadruplex formation is the ammonium (NH_4^+). A previous study reports on the influence of the cation on the G-quadruplex structure and stability.[39] Briefly, ammonium propensity to induce parallel structures is intermediate between potassium and sodium. When parallel structures are formed, their stability in ammonium is intermediate between the stability in potassium and sodium. Antiparallel structures are less stable in ammonium than in sodium and potassium.

We therefore conducted the whole study using the ammonium acetate at pH 7.0, because ammonium acetate produces volatile components upon electrospray. The peaks observed in the electrospray mass spectra give precious indications on the extent of G-quadruplex formation, because, even in complex mixtures, for each species the number of strands and the number of embedded ammonium cations can be determined. For QFOs giving rise to intramolecular G-quadruplexes, the number of ammoniums is indicative of G-quadruplex formation (the number of strands remains equal to one). In these cases ESI-MS is useful also to check for unsuspected multimolecular arrangements.[39] All the here studied quadruplexes have tracts of four consecutive guanines, so the expected number of ammonium ions for the perfect G-quadruplex is equal to three.

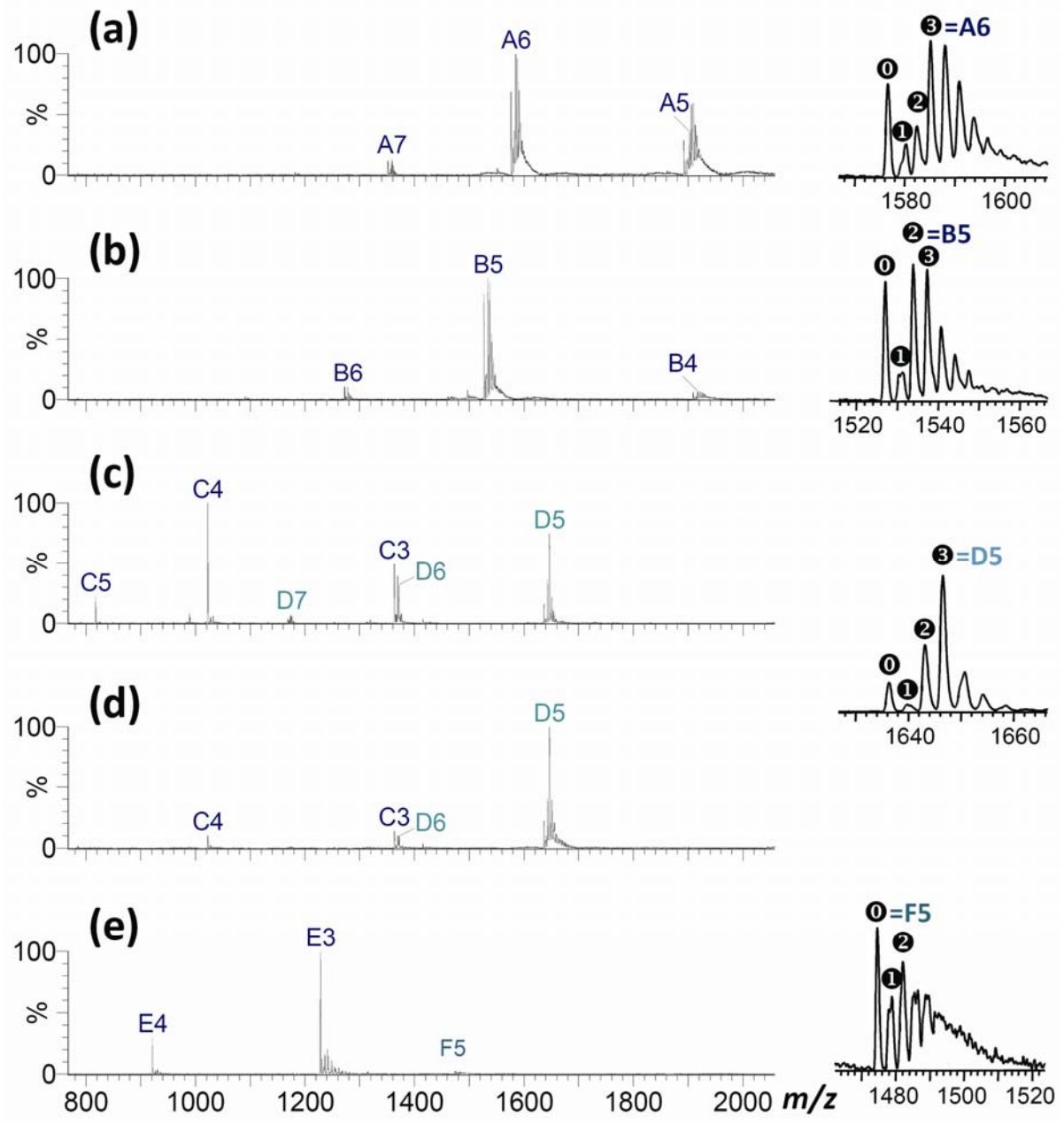

Figure 1: ESI-MS spectra of: (a) TG4T4-intra in 150 mM NH_4OAc; (b) TG4T2-intra in 150 mM NH_4OAc; (c) TG4T3-bi in 10 mM NH_4OAc; (d) TG4T3-bi in 150 mM NH_4OAc; (e) T4G4T4 in 150 mM NH_4OAc. All spectra were acquired in the following soft source conditions: RF Lens1 = 80 V; cone = 80 V; collision energy = 10 V. Zooms on the right show the distribution of the number of ammonium ions remaining in the G-quadruplexes (from 0 to 3). Major peaks are annotated with a letter indicating the component and a figure indicating the charge state. Component A =[TG4T4-intra•$(NH_4)_3$]; B = [TG4T2-intra•$(NH_4)_2$]; C = [TG4T3-bi]; D = [$(TG4T3\text{-}bi)_2$•$(NH_4)_3$]; E = [T4G4T4]; F = [$(T4G4T4)_2$].

Table 2: Summary of the peaks observed in the electrospray mass spectra of the DNA sequences (in the absence of PNA) in different solvent systems. Peaks attributed to G-quadruplexes (four guanine tracts and three ammonium cations embedded) are underlined. (m.p. = main product)

Sequence	**Observed in H_2O**	**Observed in 10 mM NH_4OAc**	**Observed in 150 mM NH_4OAc**
TG4T2-intra	$[M]^{7- \rightarrow 12-}$	$[M]^{8- \rightarrow 10-}$ $[M]^{7-} > [M(NH_4)]^{7-} > [M(NH_4)_2]^{7-}$ $[M(NH_4)_2]^{6-} > \underline{[M(NH_4)_3]^{6-}}$ $[M(NH_4)_2]^{5-} > \underline{[M(NH_4)_3]^{5-}}$	$[M]^{8- \rightarrow 10-}$ $[M]^{7-} > [M(NH_4)]^{7-} >$ $[M(NH_4)_2]^{7-}$ $[M(NH_4)_2]^{6-} > \underline{[M(NH_4)_3]^{6-}}$ $[M(NH_4)_2]^{5-} > \underline{[M(NH_4)_3]^{5-}}$
TG4T3-intra	$[M]^{6- \rightarrow 12-}$	$\underline{[M(NH_4)_3]^{4- \rightarrow 7-}}$	$\underline{[M(NH_4)_3]^{4- \rightarrow 7-}}$
TG4T4-intra	$[M]^{6- \rightarrow 12-}$	$\underline{[M(NH_4)_3]^{4- \rightarrow 7-}}$	$\underline{[M(NH_4)_3]^{4- \rightarrow 7-}}$
TG4T3-bi	$[M]^{3- \rightarrow 6-}$	$[M]^{3- \rightarrow 5-}$, m.p. $\underline{[M_2(NH_4)_3]^{5-/6-}}$	$[M]^{2-}$ $\underline{[M_2(NH_4)_3]^{4-/5-}}$, m.p.
TG4T	$[M]^{2- \rightarrow 4-}$	$[M]^{2-/3-}$ $[M_2]^{3-}$	$[M]^{2-}$ $\underline{[M_4(NH_4)_3]^{4-/5-}}$, m.p.
T4G4T4	$[M]^{3- \rightarrow 6-}$	$[M]^{3- \rightarrow 5-}$, m.p. $[M(NH_4)]^{3-} > [M(NH_4)_2]^{3-} >$ $[M(NH_4)_3]^{3-}$ $[M_2]^{5-}$	$[M]^{2--}$, m.p. $[M_2]^{4-/5-}$

ESI-MS shows that all the three intramolecular putative quadruplex sequences (PQSs) do indeed form G-quadruplexes in both 10 mM and 150 mM NH_4OAc, and no higher-order stoichiometries were detected. ESI-MS spectra were collected tuning Q-TOF for higher sensitivity, allowing higher ion density into the TOF, and as a result the resolution is < 8000. For this reason we cannot distinguish the isotopic peaks separated by 1/z. However the separation between ammonium adducts (17/z) is clearly visible, can be used to confirm the charge state. For example, the spectrum of TG4T4-intra in 150 mM NH_4OAc shown in Figure 1(a) shows that the major species is the oligonucleotide sequence with three ammonium cations embedded. Only the ESI-MS spectra of TG4T2-intra are more complex to interpret (see Figure 1(b) for TG4T2-intra in 150 mM NH_4OAc), with monomers detected with 3, 2, 1 or 0 ammoniums depending on the charge state. This can indicate two things: either the G-quadruplex is not fully formed in the injected solution, or the G-quadruplex is fully formed but the ammonium cations embedded in the desolvated ions are expelled as neutral NH_3 before the G-quadruplex ions reach the mass analyzer. Previous studies have shown that the gas-phase stability of the complex with the inner ammonium decreases as the charge state increases,[56] and when the loop constraints increase.[47] The ammonium adduct distribution of TG4T2-intra resembles the ammonium adduct distribution of the G-quadruplex $(GGGGTTTTGGGG)_2$ when slightly activated in the source.[47] For TG4T2-intra, CD and UV-melting will help proving G-quadruplex formation.

For bimolecular and tetramolecular QFOs, G-quadruplex structure formation can be assigned unambiguously using strand count (two and four strands, respectively). For example, TG4T3-bi forms a dimeric G-quadruplex which is found less abundant than the monomer peak in 10 mM NH_4OAc (Figure 1(c)), and becomes the main product at 150 mM NH_4OAc (Figure 1(d)). For the strands containing only one tract of guanines, the G-quadruplex is tetramolecular. When the

strands are stored at 50 μM (for intramolecular QFOs), 100 μM (for bimolecular QFOs) and 200 μM (for tetramolecular QFOs), in 150 mM NH_4OAc during 16 h, the G-quadruplex is the main product. For T4G4T4, however, the G-quadruplex cannot be detected, even in 150 mM NH_4OAc (see Figure 1(e)). This is due to kinetic reasons: G-quadruplex formation becomes slower as the stoichiometry of the G-quadruplex increases,[57,58] and as the cation concentration decreases. Furthermore, G-quadruplex formation in ammonium is known to be slower than in potassium or sodium cations.[59] The 16 hours allowed for quadruplex formation are not enough for TG4T in 10 mM NH_4OAc,[59] and for T4G4T4 both in 10 and 150mM NH_4OAc.

Circular Dichroism

Circular dichroism is used to indicate whether the QFOs fold into parallel or antiparallel configuration. Parallel quadruplexes display a positive CD signal around 265 nm, and a negative peak at 240 nm, while antiparallel ones exhibit a positive signal at around 295 nm, and a negative signal or shoulder around 260 nm.[31,60,61] However there is some debate about the CD signature of antiparallel and parallel G-quadruplexes, and exceptions to these rules have been reported.[62,63] Figure 2 shows the CD spectra of all six DNA sequences as recorded in H_2O, 10 mM NH_4OAc and 150 mM NH_4OAc. The CD spectra suggest that the three intramolecular G-quadruplexes TG4T2-intra, TG4T3-intra and TG4T4-intra are predominantly antiparallel in ammonium acetate.

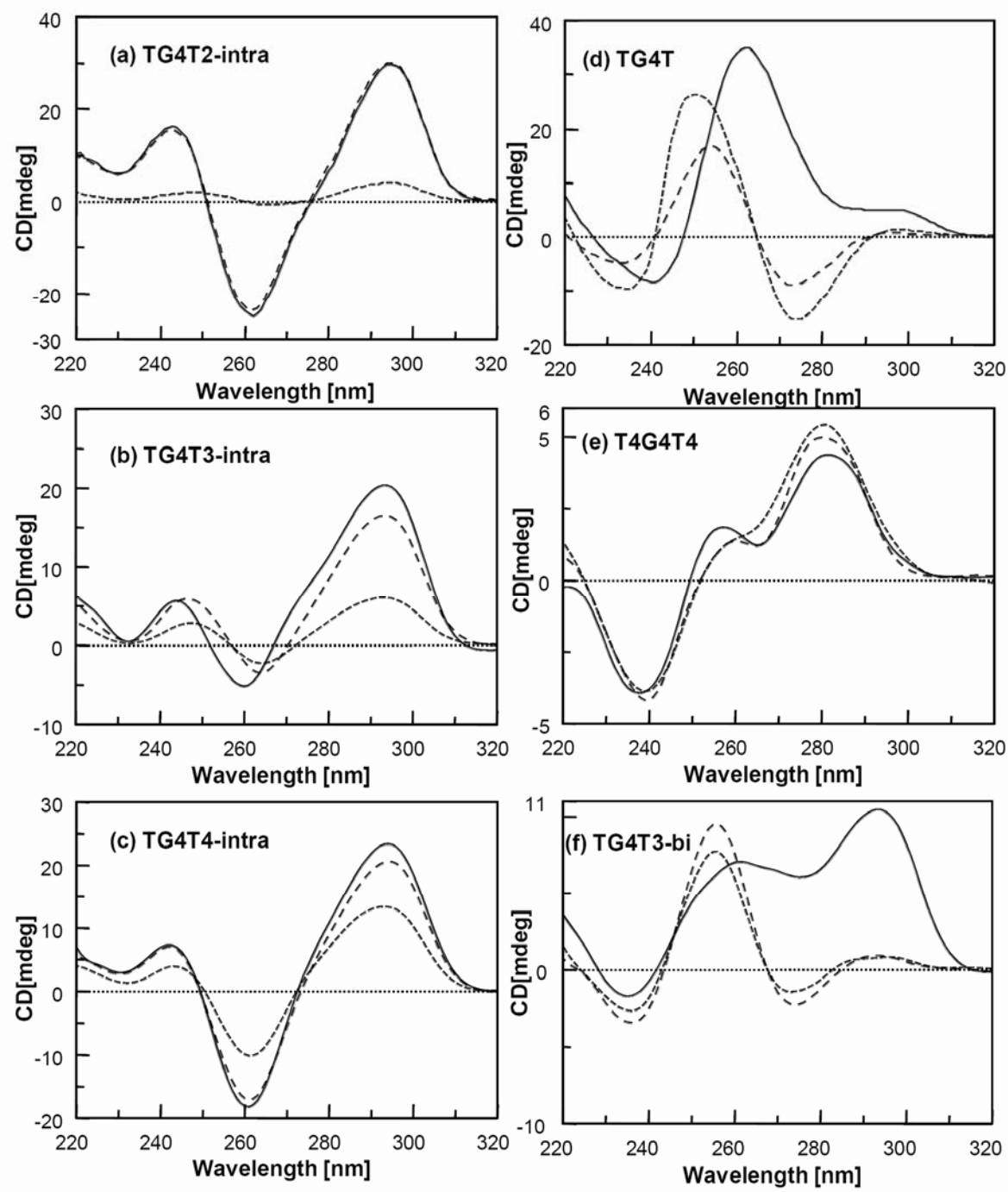

Figure 2. Circular dichroism spectra of the six DNA sequences recorded in H_2O (short dash), 10 mM NH_4OAc (long dash) and 150 mM NH_4OAc (solid line): (a) TG4T2-intra, (b) TG4T3-intra, (c) TG4T4-intra, (d) TG4T, (e) T4G4T4, (f) TG4T3-bi.

The dimeric G-quadruplex forming sequence (TG4T3-bi) shows two positive dichroic bands at 295 nm (the highest) and at 260 nm (the lowest) corresponding to a mixture of antiparallel (major) and parallel (minor) contributions. CD spectra recorded at various temperatures and CD melting profiles at 295 nm and 260 nm confirm the presence of a mixture of G-quadruplex conformations (data not shown).

TG4T shows a CD profile typical of parallel G-quadruplexes in 150 mM NH_4OAc, but not in 10 mM NH_4OAc. Again this is due to kinetic reasons: the low strand concentration (3 μM) did not allow significant amounts of G-quadruplex to form in 10 mM buffer. T4G4T4 at 3 μM did not form G-quadruplex structures at all, showing that poly-T overhangs destabilize tetramolecular G-quadruplex formation. The CD spectrum of T4G4T4 in 150 mM NH_4OAc shows only two weak positive dichroic bands at 282 nm (major) and at 256 nm (minor). When recorded for the same sample after warming at 90 °C for 1h, the CD spectrum shows that the maximum at 282 nm shifts to 278 nm, while the weak positive band at 256 nm disappears.

The CD band centered at 256 nm is not characteristic of a quadruplex structure, but it is temperature dependent, indicating that it corresponds to a DNA secondary structure. It was then checked in the ESI-MS whether other possible secondary structures in TG4T (10 mM NH4OAc) and T4G4T4 could be detected. The common feature of these MS spectra is the presence of dimers (instead of the tetrameric quadruplex). For example, $[(T4G4T4)_2 \bullet (NH_4)_{0\text{-}2}]^{4-/5-}$ is detected (see inset of Figure 1(e)), along with the most abundant single strand. The CD band at 256 nm could therefore tentatively be ascribed to pairing interactions between G-tracts.

Thermal denaturation

In agreement with the behavior observed in CD experiments, UV melting profiles recorded at 295 nm suggest quadruplex formation in 150 mM NH_4OAc for all the sequences, except for T4G4T4. In the case of TG4T3-bi in 150 mM NH_4OAc, we can observe two transitions in the UV melting profile at 295 nm. As the CD profile showed two positive dichroic bands at 295 nm and at 261 nm, we performed also CD melting experiments for TG4T3-bi in 150 mM NH_4OAc at 261 nm and at 295 nm (see Supporting Information). Two transitions are observable in the curve recorded at 261 nm, for this reason the positive dichroic band at 261 nm could correspond to a mixture of structures. The CD melting profile at 295 nm shows a transition with a T_m = 60 °C, like the major transition observed in UV-vis. In conclusion, TG4T3-bi in 150 mM NH_4OAc forms a complex mixture of parallel and antiparallel quadruplexes.

Table 3: Melting temperatures of the DNA sequences (in the absence of PNA) in different solvent systems. All were determined by UV absorbance monitored at 295 nm.

Sequence	**T_m in 10 mM NH_4OAc**	**T_m in 150 mM NH_4OAc**
TG4T2-intra	42 °C	61 °C
TG4T3-intra	24 °C (1/3) and 57 °C (2/3)	63 °C
TG4T4-intra	37 °C (1/2) and 54 °C (1/2)	68 °C
TG4T3-bi	-	75 °C
TG4T	-	77 °C
T4G4T4	-	34 °C (1/5) and 60 °C (4/5)

In 10 mM NH_4OAc, G-quadruplex formation is observed only in the case of intramolecular QFOs, while in the same conditions UV melting spectra recorded for intermolecular QFOs confirm their absence. Again, this is due to kinetic reasons: the G-quadruplexes do not have enough time to form at that low strand concentration (3 μM). Furthermore, the UV-melting curves for TG4T3-intra and TG4T4-intra show two transitions, suggesting also a mixture of conformations, which is no longer the case at 150 mM NH_4OAc.

Interaction of QFOs with [acccca]-PNA

Multiple PNA adducts on linear QFOs

Electrospray mass spectrometry was used to investigate the various complex stoichiometries that can be formed between the QFOs containing one, two or four dTGGGGT units and the short [acccca]-PNA. Three different solvents were tested: bi-distilled H_2O, 10 mM NH_4OAc and 150 mM NH_4OAc. Furthermore, for the ammonium acetate solutions, two types sample preparation procedures were tested: the PNA and QFO were mixed either at room temperature (with a G-quadruplex that was allowed to form for 24 h), or at 90 °C where the G-quadruplex structure is disrupted (see materials and methods for details). As we shall see below, the preparation procedure influences the resulting complexes, even though the final concentrations and temperature are the same. Table 4 summarizes the major species identified from the mass spectra, which turned out to be particularly rich.

Table 4: Summary of the peaks observed in the electrospray mass spectra of the DNA-PNA mixtures in different solvent systems. Peaks attributed to G-quadruplex folded structures are underlined. (M = DNA in single stranded form; mp = main products)

Sequence	**H_2O**	**10 mM NH_4OAc, 90° mix**	**150 mM NH_4OAc, 90° mix**	**10 mM NH_4OAc, RT mix**	**150 mM NH_4OAc, RT mix**
TG4T2-intra	$[M•(PNA)_4]^{6-\rightarrow 10-}$ mp $[M•(PNA)_5]^{5-\rightarrow 10-}$ $[M_2•(PNA)_8]^{9-\rightarrow 14-}$ mp $[M_2•(PNA)_{10}]^{10-\rightarrow 16-}$ $[M_2•(PNA)_{11}]^{10-\rightarrow 14-}$ $[M_2•(PNA)_{12}]^{10-\rightarrow 16-}$ $[M_3•(PNA)_{16}]^{14-\rightarrow 19-}$	$[M•(PNA)_3]^{6-\rightarrow 8-}$ $[M•(PNA)_4]^{5-\rightarrow 9-}$ $[M•(PNA)_5]^{5-\rightarrow 10-}$ $[M_2•(PNA)_{10}]^{10-\rightarrow 16-}$ mp $[M_2•(PNA)_{11}]^{10-\rightarrow 14-}$ $[M_2•(PNA)_{12}]^{10-\rightarrow 16-}$ $[M_3•(PNA)_{16}]^{14-\rightarrow 19-}$	$\underline{[M(NH_4)_{2/3}]^{5-/6-}}$ mp $[M•(PNA)_4]^{6-/7-}$ $[M•(PNA)_5]^{6-\rightarrow 8-}$	$\underline{[M(NH_4)_{2-3}]^{5-}}$ $\underline{[M(NH_4)_{2-3}•M•(PNA)_4]^{9-\rightarrow 15-}}$ mp $\underline{[M(NH_4)_{2-3}•M•(PNA)_5]^{10-\rightarrow 13-}}$ $\underline{[M(NH_4)_{2-3}•M•(PNA)_6]^{10-\rightarrow 12-}}$	$\underline{[M(NH_4)_{2-3}]^{5-/6-}}$ $\underline{[M(NH_4)_{1-2}•PNA]^{5-/6-}}$
TG4T3-intra	$[M•(PNA)_4]^{8-\rightarrow 12-}$	$[M•(PNA)_4]^{7-/8-}$ mp $[M•(PNA)_5]^{6-\rightarrow 8-}$ $[M•(PNA)_6]^{7-/8-}$	$\underline{[M(NH_4)_3]^{5-\rightarrow 7-}}$ mp $[M•(PNA)_4]^{6-/7-}$	$\underline{[M(NH_4)_3]^{5-\rightarrow 7-}}$ mp $\underline{[M(NH_4)_2•PNA]^{5-\rightarrow 8-}}$	$\underline{[M(NH_4)_3]^{5-\rightarrow 7-}}$ mp $\underline{[M(NH_4)_2•PNA]^{5-/6-}}$
TG4T4-intra	$[M•(PNA)_4]^{7-\rightarrow 15-}$ mp $[M•(PNA)_5]^{7-\rightarrow 13-}$ $[M•(PNA)_6]^{6-\rightarrow 16-}$ mp $[M_2•(PNA)_{12}]^{11-\rightarrow 15-}$	$[M•(PNA)_2]^{6-\rightarrow 9-}$ $[M•(PNA)_4]^{7-\rightarrow 13-}$ $[M•(PNA)_5]^{6-\rightarrow 12-}$ $[M•(PNA)_6]^{6-\rightarrow 11-}$ mp $[M_2•(PNA)_{11}]^{11-\rightarrow 15-}$ $[M_2•(PNA)_{12}]^{11-\rightarrow 15-}$	$\underline{[M(NH_4)_3]^{5-/6-}}$ $[M•(PNA)_2]^{5-\rightarrow 8-}$ mp $[M•(PNA)_3]^{6-\rightarrow 9-}$ $[M•(PNA)_4]^{6-\rightarrow 8-}$ $[M•(PNA)_5]^{6-\rightarrow 9-}$ $[M•(PNA)_6]^{6-\rightarrow 9-}$ (+ small free PNA)	$\underline{[M(NH_4)_3]^{6-/7-}}$ $\underline{[M(NH_4)_3•PNA]^{6-\rightarrow 9-}}$ mp $\underline{[M(NH_4)_3•(PNA)_2]^{6-\rightarrow 8-}}$ $[M_2•(PNA)_8]^{10-\rightarrow 15-}$ $[M_2•(PNA)_9]^{11-\rightarrow 15-}$ $[M_2•(PNA)_{10}]^{11-\rightarrow 15-}$ $[M_2•(PNA)_{11}]^{12-\rightarrow 15-}$	$\underline{[M(NH_4)_3]^{5-\rightarrow 7-}}$ mp $\underline{[M(NH_4)_3•PNA]^{5-/6-}}$ $\underline{[M(NH_4)_3•(PNA)_2]^{6-/7-}}$ (+ large free PNA)
TG4T3-bi	$[M]^{4-/5-}$ $[M•PNA]^{3-\rightarrow 6-}$ $[M•(PNA)_2]^{3-\rightarrow 7-}$ mp $[M•(PNA)_3]^{3-\rightarrow 8-}$ $[M•(PNA)_4]^{3-\rightarrow 7-}$ $[M_2•(PNA)_4]^{6-\rightarrow 10-}$	$[M•PNA]^{3-\rightarrow 6-}$ $[M•(PNA)_2]^{3-\rightarrow 7-}$ mp $[M•(PNA)_3]^{3-\rightarrow 7-}$ mp $[M_2•(PNA)_2]^{5-\rightarrow 10-}$ $[M_2•(PNA)_4]^{6-\rightarrow 8-}$ $[M_2•(PNA)_5]^{5-\rightarrow 9-}$	$[M]^{3-\rightarrow 5-}$ $[M•PNA]^{3-\rightarrow 5-}$ $[M•(PNA)_2]^{3-\rightarrow 6-}$ $[M•(PNA)_3]^{3-\rightarrow 6-}$ $[M_2•(PNA)_2]^{4-\rightarrow 7-}$ $[M_2•(PNA)_3]^{5-\rightarrow 8-}$	$[M]^{4-/5-}$ (+ large free PNA) $[M•PNA]^{3-\rightarrow 6-}$ mp $\underline{[M_2(NH_4)_{0-3}•PNA]^{5-/6-}}$ $\underline{[M_2(NH_4)_{0-3}•(PNA)_2]^{5-\rightarrow 7-}}$ $\underline{[M_2(NH_4)_{0-3}•(PNA)_3]^{6-}}$ $\underline{[M_2(NH_4)_3•M•(PNA)_4]^{8-\rightarrow 11-}}$	$[M]^{3-/4-}$ $\underline{[M_2(NH_4)_3]^{5-/6-}}$ $\underline{[M_2(NH_4)_3•PNA]^{5-/6-}}$ $\underline{[M_2(NH_4)_3•(PNA)_2]^{6-}}$

	$[M_2•(PNA)_5]^{5-\rightarrow 10-}$ $[M_2•(PNA)_6]^{6-\rightarrow 10-}$ $[M_3•(PNA)_8]^{7-\rightarrow 13-}$	$[M_2•(PNA)_6]^{6-\rightarrow 10-}$ $[M_3•(PNA)_8]^{8-\rightarrow 13-}$ $[M_4•(PNA)_9]^{10-\rightarrow 12-}$ $[M_4•(PNA)_{10}]^{10-\rightarrow 14-}$ $[M_4•(PNA)_{11}]^{11-\rightarrow 11-}$	$[M_3•(PNA)_5]^{7-/8-}$	$\underline{[M_2(NH_4)_3•M•(PNA)_5]^{8-\rightarrow 10-}}$ $\underline{[M_2(NH_4)_3•M•(PNA)_6]^{8-\rightarrow 10-}}$	
TG4T	No peaks	$[M]^{2-/3-}$ and $[PNA]^{1-/2-}$ mp $[M•PNA]^{2-\rightarrow 4-}$ mp $[M•(PNA)_2]^{3-/4-}$ $[M_2•PNA]^{3-/4-}$	$[M]^{1-\rightarrow 3-}$ and $[PNA]^{1-/2-}$ $[M•PNA]^{2-\rightarrow 5-}$ mp $[M•(PNA)_2]^{3-/4-}$ $[M_2•PNA]^{3-/4-}$	$[M]^{2-/3-}$ and $[PNA]^{1-/2-}$ $\underline{[M(NH_4)_{2-3}]^{5-}}$ $[M•PNA]^{2-/3-}$ mp $[M•(PNA)_2]^{3-/4-}$ $[M_2•PNA]^{3-/4-}$ $[M_2•(PNA)_2]^{3-}$ $[M_2•(PNA)_3]^{4-}$ $[M_3•(PNA)_2]^{4-}$ $[M_3•(PNA)_2]^{5-}$	$[M•PNA]^{2-/3-}$ $[M•(PNA)_2]^{2-\rightarrow 4-}$ $\underline{[M_4(NH_4)_3]^{3-\rightarrow 6-}}$ $\underline{[M_4(NH_4)_3•PNA]^{4-\rightarrow 6-}}$ $\underline{[M_4(NH_4)_3•(PNA)_2]^{5-}}$ $\underline{[(M_4(NH_4)_3)_2]^{7-}}$ $\underline{[(M_4(NH_4)_3)_2•PNA]^{6-/7-}}$ $\underline{[(M_4(NH_4)_3)_2•(PNA)_2]^{7-/8-}}$
T4G4T4	$[M]^{3-\rightarrow 5-}$ $[M•PNA]^{3-\rightarrow 6-}$ $[M•(PNA)_2]^{3-\rightarrow 7-}$ mp $[M•(PNA)_3]^{3-\rightarrow 7-}$ $[M•(PNA)_4]^{4-\rightarrow 6-}$ $[M_2•(PNA)_4]^{5-\rightarrow 11-}$ $[M_2•(PNA)_5]^{5-\rightarrow 10-}$ $[M_2•(PNA)_6]^{5-}$ $[M_3•(PNA)_6]^{5-\rightarrow 13-}$ $[M_4•(PNA)_8]^{8-\rightarrow 13-}$ $[M_5•(PNA)_{10}]^{10-\rightarrow 13-}$	$[M]^{3-\rightarrow 5-}$ $[M•PNA]^{3-\rightarrow 7-}$ mp $[M•(PNA)_2]^{3-\rightarrow 7-}$ mp $[M•(PNA)_3]^{3-\rightarrow 6-}$ $[M_2•(PNA)_3]^{5-\rightarrow 9-}$ $[M_2•(PNA)_4]^{5-\rightarrow 11-}$ $[M_2•(PNA)_5]^{5-\rightarrow 11-}$ $[M_3•(PNA)_5]^{7-\rightarrow 9-}$ $[M_3•(PNA)_6]^{7-\rightarrow 11-}$	$[M]^{3-\rightarrow 5-}$ $[M•PNA]^{3-\rightarrow 6-}$ mp $[M•(PNA)_2]^{3-\rightarrow 6-}$ $[M_2•(PNA)_2]^{4-\rightarrow 6-}$ $[M_2•(PNA)_3]^{5-\rightarrow 7-}$ $[M_2•(PNA)_4]^{5-\rightarrow 8-}$	$[M]^{3-\rightarrow 5-}$ $[M•PNA]^{3-\rightarrow 6-}$ $[M•(PNA)_2]^{3-\rightarrow 8-}$ mp $[M•(PNA)_3]^{4-\rightarrow 7-}$ $[M•(PNA)_4]^{4-\rightarrow 6-}$ $[M_2•(PNA)_4]^{5-\rightarrow 11-}$ $[M_2•(PNA)_5]^{5-\rightarrow 9-}$ $[M_3•(PNA)_6]^{7-\rightarrow 11-}$ $[M_3•(PNA)_7]^{8-\rightarrow 11-}$ $[M_3•(PNA)_8]^{7-\rightarrow 10-}$	$[M•PNA]^{3-\rightarrow 6-}$ mp $[M•(PNA)_2]^{3-\rightarrow 6-}$ $[M•(PNA)_3]^{4-/5-}$ $[M•(PNA)_4]^{4-\rightarrow 6-}$ $[M_2•(PNA)_3]^{5-\rightarrow 7-}$ $[M_2•(PNA)_4]^{6-\rightarrow 8-}$ $[M_2•(PNA)_5]^{6-/7-}$

With unfolded QFOs, we anticipated the formation of short complementary DNA•PNA duplexes along the DNA sequence, and hence [M•$(PNA)_n$] complexes (*n* being the number of TGGGGT units in the QFO). In H_2O, the major complex formed with the QFOs containing *n* dTGGGGT units is usually the [M•$(PNA)_n$] complex, corresponding to one [acccca]-PNA per dTGGGGT unit, but in addition, [M•$(PNA)_{n+1}$] and [M•$(PNA)_{n+2}$] are also observed, indicating that short DNA•$(PNA)_2$ triplexes can also be formed. The same results are obtained in 10 mM and 150 mM NH_4OAc when the mixing was done at 90 °C, indicating that upon cooling, DNA•PNA duplex formation is faster than G-quadruplex formation. The duplex/triplex ratio depends on the salt concentration, as illustrated in Figure 3 for T4G4T4 which contains only one TGGGGT unit. The duplex [M•PNA] (noted A in Figure 3) is favored at high ionic strength, and the triplex [M•$(PNA)_2$] (noted B in Figure 3) is favored at low ionic strength. Low ionic strength stabilizes hydrogen bonds. Because the triplex formation requires a greater number of hydrogen bonds triplex is favored at low ionic strength, while high ionic strength gives a greater amount of heteroduplexes.

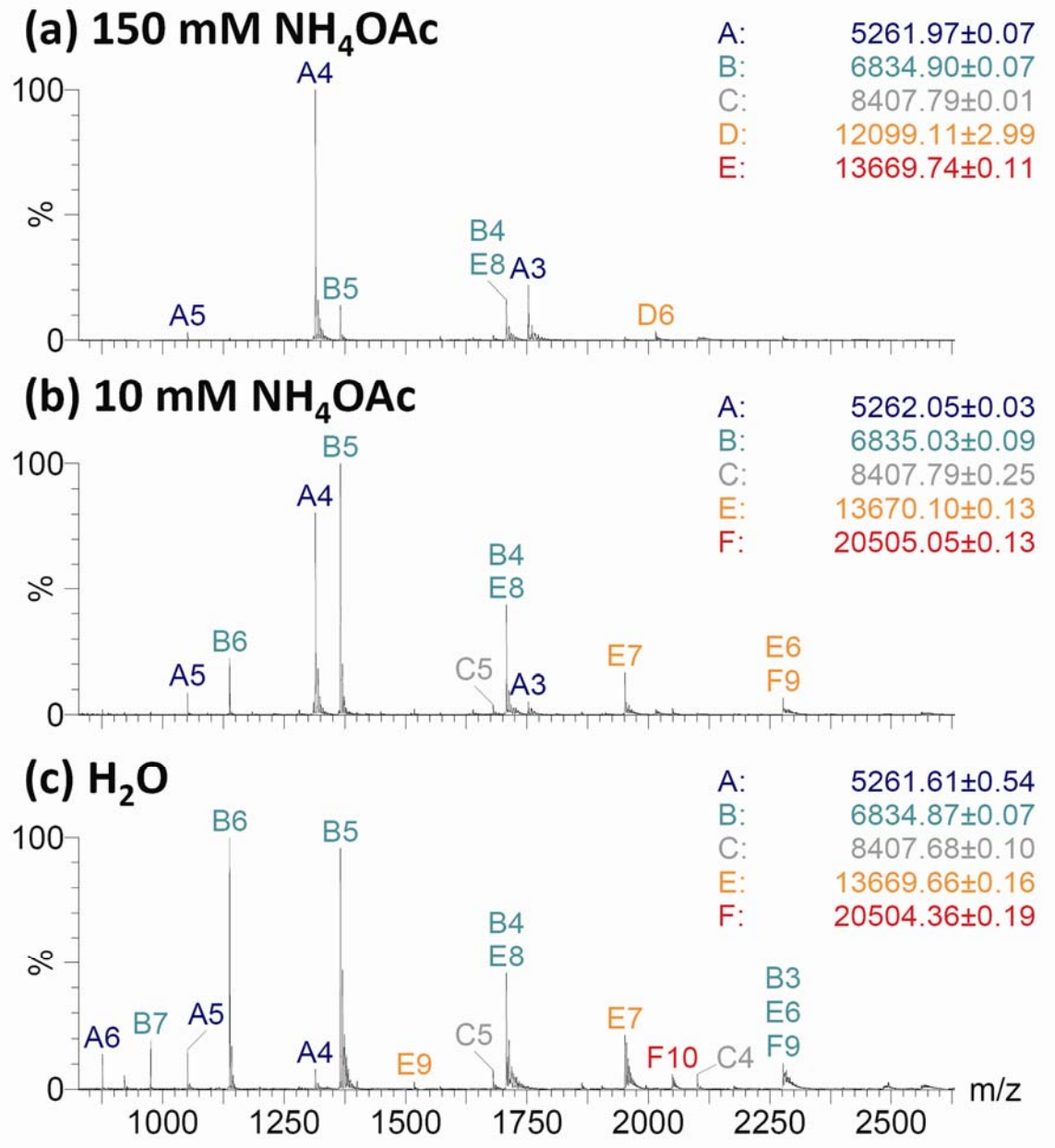

Figure 3: ESI-MS spectra of T4G4T4 (10 μM) + PNA (10 μM) in (a) 150 mM NH_4OAc prepared by mixing at 90 °C, (b) 10 mM NH_4OAc prepared by mixing at 90 °C and (c) H_2O. Mass spectrometer settings: RF Lens1 = 120 V; cone = 80 V; collision energy = 15 V. Major peaks are annotated with a letter indicating the component and a figure indicating the charge state. Component A = [M•PNA] (theoretical mass = 5261.96 Da); B = [M•$(PNA)_2$] (6835.48 Da); C = [M•$(PNA)_3$] (8409.00 Da); D = [M_2•$(PNA)_3$] (12097.44 Da); E = [M_2•$(PNA)_4$] (13670.96 Da); F = [M_3•$(PNA)_6$] (20506.44 Da).

Higher-order structure formation and aggregation at low ionic strength

Clues for early aggregation intermediates can be seen in the ESI-MS spectra obtained for various sequences. For example, in the aqueous spectra of T4G4T4, $[M_n•(PNA)_{2n}]$ complexes are detected with *n* up to 5 (component L in Figure 4(a)). TG4T2-intra also showed unanticipated stoichiometries (Figure 4(b)), with $[M_2•(PNA)_{10}]^{10-\rightarrow16-}$ (component D) being the main product, and $[M_3•(PNA)_{16}]$ (component G) being a significant component of the mixture.

Another interesting case is that of the short TG4T 6-mer that is exactly complementary to the PNA. In H_2O, no mass spectrum can be obtained, and a white gel is formed in the solution. However, when 10 mM NH_4OAc is added to that gel, the solution becomes limpid and the ESI-MS spectrum shows clearly the [M•PNA] complex.

For longer sequences, aggregation in pure water did not occur if the DNA sequences undergo only a simple desalting, and the ESI-MS spectra show detectable peaks. Figure 5a shows the ESI-MS spectrum recorded in H_2O for TG4T3-intra + PNA, when the DNA was prepared with one passage on Microcon 5 kDa filters. Only $[M•(PNA)_4]$ is observed, suggesting again a structure with four short duplexes like beads on a string. The high-mass peak broadening is attributed to sodium and potassium adducts. The experiment was therefore repeated with extensive desalting before mixing with PNA. In that case, a precipitate forms immediately upon PNA addition, and the ESI-MS spectrum shows no peaks (Figure 5b). Finally, if ammonium acetate is added at room temperature to the precipitate to obtain a final concentration of 10 mM NH_4OAc, peaks reappear in the MS spectra (Figure 5c), corresponding to the G-quadruplex and quadruplex•PNA complex (see next paragraph). Ammonium acetate therefore redissolves the DNA•PNA precipitate. Overall, our results demonstrate that complementary PNA and DNA

aggregate at very low ionic strength, and the PNA complexes with the unfolded DNA become soluble by the addition of even low amounts of salts.

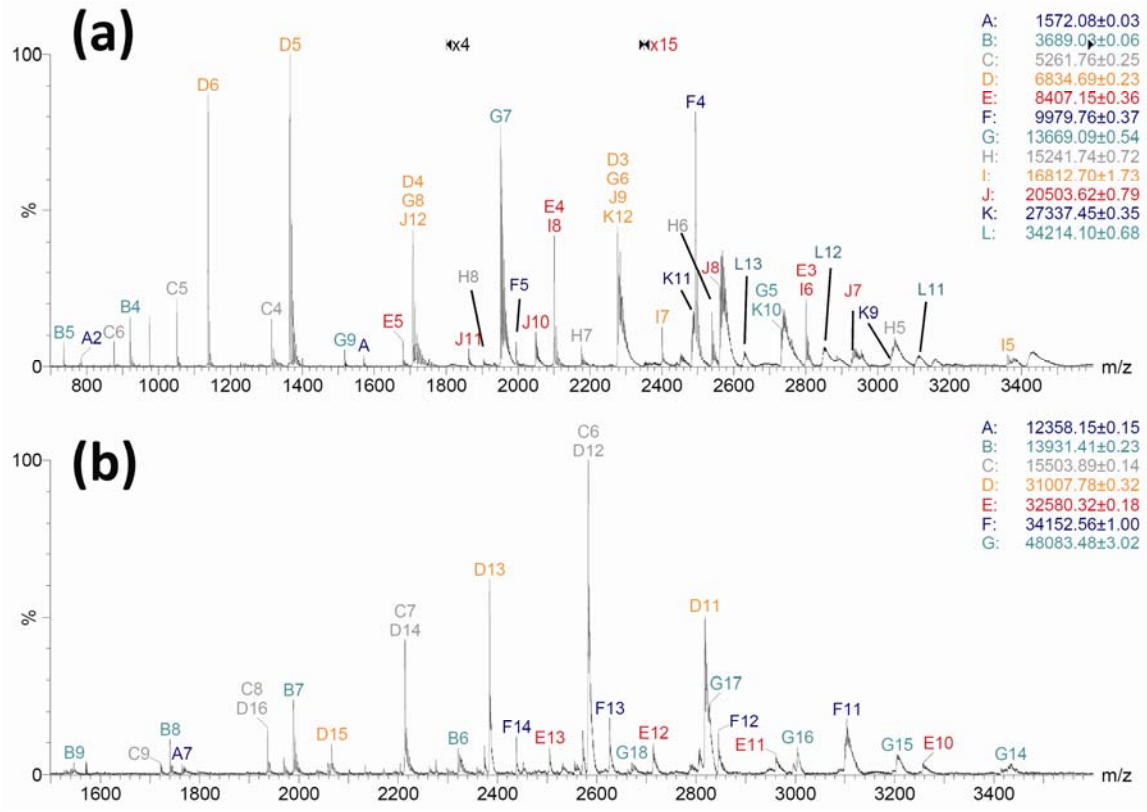

Figure 4: ESI-MS spectra of (a) 10 µM T4G4T4 + 10 µM PNA in H_2O, and (b) 10 µM TG4T2-intra + 40 µM PNA in 10 mM NH_4OAc, prepared by mixing at 90 °C. The spectrum is a sum of scans recorded at various voltage settings in order to display all peaks simultaneously (see experimental section). Note the zooms (× 4 from 1800 to 2350, and × 15 from 2350 to 3600) in panel (a). Major peaks are annotated with the letter referring to the component table on the right (average mass unless specified otherwise) and the number indicating the charge state. Panel (a): Component A = [PNA] (theoretical mass = 1572.64 Da, monoisotopic mass); B = [M] (3688.44 Da); C = [M•PNA] (5261.96 Da); D = [M•$(PNA)_3$] (6835.48 Da); E = [M•$(PNA)_3$] (8409.00 Da); F = [M•$(PNA)_4$] (9982.52 Da); G = [M_2•$(PNA)_4$] (13670.96 Da); H = [M_2•$(PNA)_5$] (15244.48 Da); I = [M_2•$(PNA)_6$] (16818.00 Da); J = [M_3•$(PNA)_6$] (20506.44 Da); K = [M_4•$(PNA)_8$] (27341.92 Da); L = [M_5•$(PNA)_{10}$•Na_2] (34221.40 Da). Panel (b): Component A = [M•$(PNA)_3$] (theoretical mass = 12359.51 Da); B = [M•$(PNA)_4$] (13933.03 Da); C = [M•$(PNA)_5$] (15506.55 Da); D = [M_2•$(PNA)_{10}$] (31013.10 Da); E = [M_2•$(PNA)_{11}$] (32586.62 Da); F = [M_2•$(PNA)_{12}$] (34160.14 Da); G = [M_3•$(PNA)_{16}$] (48093.17 Da).

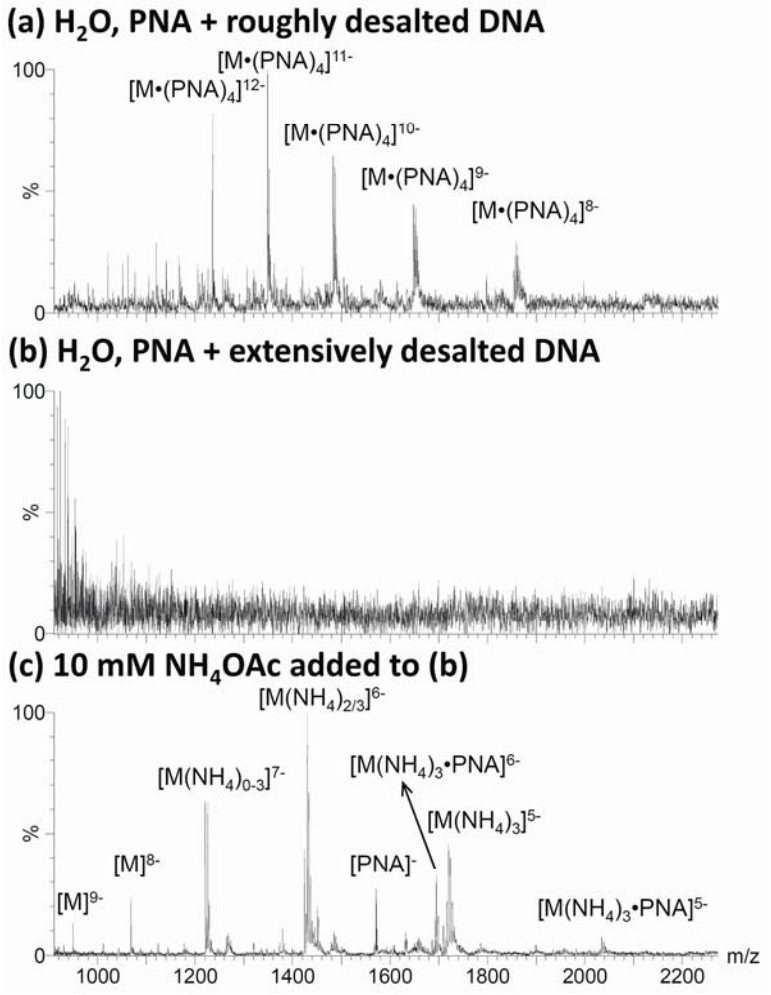

Figure 5: ESI-MS spectra of TG4T3-intra (10 μM) + PNA (40 μM) prepared as follows: (a) DNA was roughly desalted by one passage on a Microcon 5 kDa filter, then mixed with the PNA in water. (b) DNA was extensively desalted by several passages on Microcon 10 kDa filter, then mixed with PNA in water. (c) NH_4OAc was added at room temperature to the sample analyzed in (b) until a final concentration of 10 mM ammonium acetate is obtained. RF Lens1 = 80 V; cone = 80 V; collision energy = 10 V.

PNA binding to folded QFOs

When PNA is mixed at room temperature with the QFOs that were previously allowed to fold in G-quadruplex for 24h in 150 mM ammonium acetate (last column in Table 4), the major complex formed is single PNA binding to the G-quadruplex. The complex with two PNAs with

the G-quadruplex is much less abundant, but usually detected. An example is shown in Figure 6a for TG4T4-intra. In the case of the tetramolecular QFOs TG4T and T4G4T4, where 24 h is not long enough to allow complete G-quadruplex formation, the corresponding duplexes are detected along with (TG4T) or instead of (T4G4T4) the G-quadruplex. For all intramolecular and the bimolecular G-quadruplexes, we noticed that (at equivalent total charge) the inner ammonium cations in the G-quadruplex•PNA complexes were slightly less stable than in the G-quadruplex alone, but no G-quadruplex unfolding into linear structures with *n* duplexes occurs. The short PNA strands are therefore not capable of unfolding the G-quadruplexes.

When PNA is added to pre-formed G-quadruplex in 10 mM NH_4OAc, some strand aggregation is observed in addition to G-quadruplex binding: several minor peaks correspond to complexes containing one G-quadruplex with its ammoniums, one additional DNA strand, and several PNA strands. Like for the PNA complexes with the unfolded DNA, these higher-order structures disappear at higher ionic strength (150 mM NH_4OAc).

The most striking result is the dramatic difference in species formed when different preparation procedures are used: when PNA is mixed with DNA in ammonium acetate at 90 °C instead of with pre-formed G-quadruplex at room temperature, PNA•DNA duplexes with the unfolded DNA are formed instead of G-quadruplexes. See for example in Figure 6b the ESI-MS spectrum recorded for the same sample composition as in Figure 6a, except that mixing was done at 90 °C. This shows that, even for intramolecular G-quadruplexes that are known to fold quickly, short DNA•PNA duplex formation successfully competes with G-quadruplex formation upon cooling. This means that the duplex becomes stable at higher temperature than the G-quadruplex. However, the experiment consisting in redissolving the DNA-PNA precipitate using ammonium

acetate at room temperature (see preceding paragraph and Figure 5) suggests that the G-quadruplexes are the most stable species at room temperature. Overall, the system explored here therefore opens the door to new ways of creating novel PNA-DNA assemblies and modulating them by changing the experimental conditions such as ionic strength, strand concentration, and temperature.

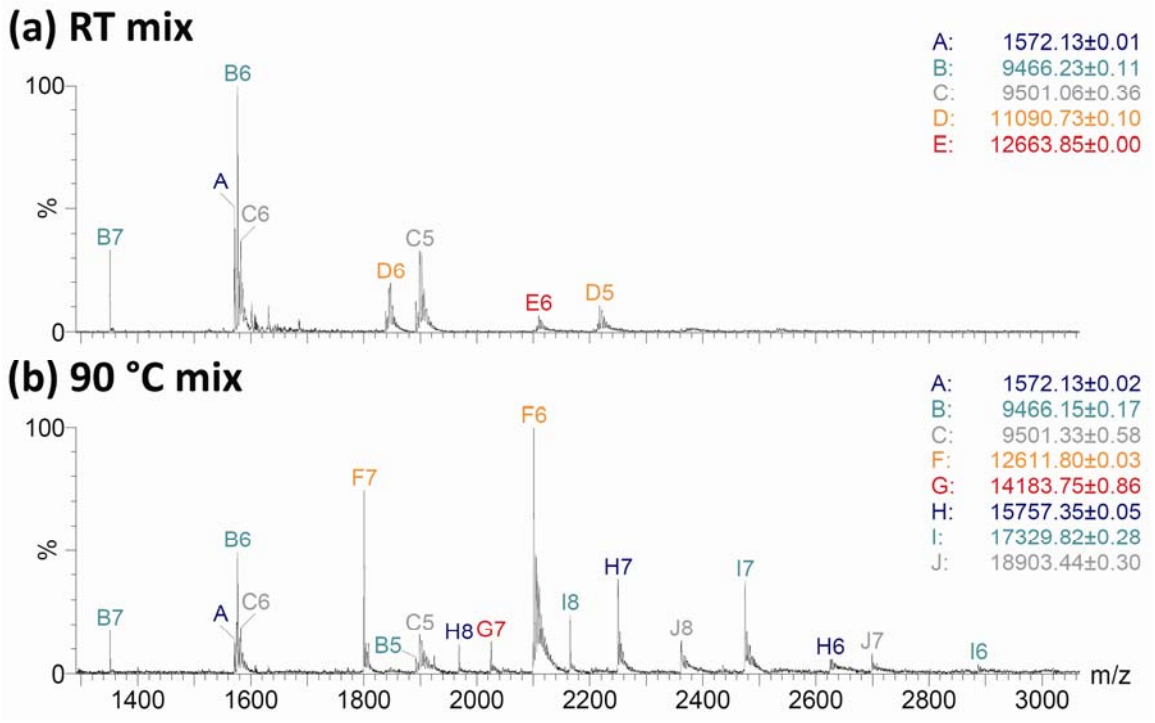

Figure 6: ESI-MS spectra of TG4T4-intra (10 μM) + PNA (40 μM) in 150 mM NH_4OAc prepared with two different procedures: (a) RT mixing and (b) mixing at 90 °C (see experimental section for details). For both spectra, mass spectrometer settings were: RF Lens1 = 120 V; cone = 80 V; collision energy = 15 V. Major peaks are annotated with a letter indicating the component and a figure indicating the charge state. Component A = [PNA] (theoretical mass = 1572.64 Da); B = [M] (9464.13 Da); C = $[M(NH_4)_2]$ (9498.13 Da); D = $[M(NH_4)_3•PNA]$ (11088.65 Da); E = $[M(NH_4)_3•(PNA)_2]$ (12662.17 Da); F = $[M•(PNA)_2]$ (12611.17 Da); G = $[M•(PNA)_3]$ (14184.69 Da); H = $[M•(PNA)_4]$ (15758.21 Da); I = $[M•(PNA)_5]$ (17331.73 Da); J = $[M•(PNA)_6]$ (18905.25 Da).

Conclusions

This study illustrates the use of electrospray mass spectrometry for investigating the varied complex stoichiometries formed between G-rich oligonucleotides and a short complementary PNA. For characterizing those systems, we fully used the power of ESI-MS for resolving the many different species at equilibrium in the system, using low amounts of sample (typically 50 µL/analysis) at micromolar concentrations. The main results concerning PNA-QFO interactions are as follows:

1) The short [ac$_4$a]-PNA is able to bind to pre-formed intramolecular, bimolecular, and tetramolecular G-quadruplexes containing four (TG_4T) repeats. Short PNAs can therefore constitute a novel type of G-quadruplex ligands. Future studies will be carried out to determine the PNA binding mode, and to investigate the influence of the PNA sequence on the binding specificity.

2) The short [ac$_4$a]-PNA is also able to bind to linear forms of the QFOs containing (TG_4T) repeats, by forming strings of short duplexes. The formation of these linear complexes however requires that no G-quadruplex is pre-formed. They can be prepared in water at room temperature, or at high ionic strength provided that the G-quadruplex is destroyed by heating at the moment of PNA addition.

3) Higher-order structures involving several DNA strands and multiple PNA binding are observed at low ionic strength. These structures possibly involve DNA-$(PNA)_2$ triplex units. Precipitation is even observed if DNA is extensively desalted before PNA mixing. Counterions are therefore extremely important in modulating DNA-PNA assembly, because they influence both aggregation of several duplexes and formation of G-

quadruplexes. Our preliminary results allow anticipating the elaboration of novel nucleic acid-based architectures, switches, or sensors that can easily be modulated by counterions and temperature.

Acknowledgements

This work was financed by the Fonds de la Recherche Scientifique-FNRS (FRFC n° 2.4.623.05 to EDP), the University of Liège (Starting grant FNRS-08/10 to VG), and a PRIN-MURST grant (2007-2010, to GO and JA). VG is a FNRS Research Associate.

References

1. Burge, S.; Parkinson, G. N.; Hazel, P.; Todd, A. K.; Neidle, S. Nucleic Acids Res 2006, 34, 5402-5415.
2. Simonsson, T. Biol Chem 2001, 382, 621-628.
3. Davis, J. T. Angew Chem Int Ed 2004, 43, 668-698.
4. Phan, A.-T.; Kuryavyi, V.; Patel, D. J. Curr Opin Struct Biol 2006, 16, 288-298.
5. Patel, D. J.; Phan, A. T.; Kuryavyi, V. Nucleic Acids Res 2007, 35, 7429-7455.
6. Riou, J.-F.; Gomez, D.; Morjani, H.; Trentesaux, C. In Quadruplex Nucleic Acids, Neidle, S., Balasubramanian, S., Eds.; The Royal Soceity of Chemistry, Cambridge, 2006; Chapter 6, 154-179.
7. Sen, D.; Gilbert, W. Nature 1988, 334, 364-366.
8. Chen, J. P.; Spector, M. S.; Kunos, G.; Gao, B. Journal of Biological Chemistry 1997, 272, 23144-23150.
9. Rangan, A.; Fedoroff, O. Y.; Hurley, L. H. J Biol Chem 2001, 276, 4640-4646.
10. Dai, J.; Dexheimer, T. S.; Chen, D.; Carver, M.; Ambrus, A.; Jones, R. A.; Yang, D. J Am Chem Soc 2006, 128, 1096-1098.
11. Dexheimer, T. S.; Fry, M.; Hurley, L. H. In Quadruplex Nucleic Acids, Neidle, S., Balasubramanian, S., Eds.; The Royal Soceity of Chemistry, Cambridge, 2006; Chapter 7, 180-207.

12. Todd, A. K.; Haider, S. M.; Parkinson, G. N.; Neidle, S. Nucleic Acids Res 2007, 35, 5799-5808.

13. Dempsey, L. A.; Sun, H.; Hanakahi, L. A.; Maizels, N. J Biol Chem 1999, 274, 1066-1071.

14. Rezler, E. M.; Bearss, D. J.; Hurley, L. H. Annu Rev Pharmacol Toxicol 2003, 43, 359-379.

15. Wang, K. Y.; McCurdy, S.; Shea, R. G.; Swaminathan, S.; Bolton, P. H. Biochemistry 1993, 32, 1899-1904.

16. Pileur, F.; Andreola, M. L.; Dausse, E.; Michel, J.; Moreau, S.; Yamada, H.; Gaidamakov, S. A.; Crouch, R. J.; Toulme, J. J.; Cazenave, C. Nucleic Acids Res 2003, 31, 5776-5788.

17. Chou, S. H.; Chin, K. H.; Wang, A. H. J. Trends Biochem Sci 2005, 30, 231-234.

18. Girvan, A. C.; Teng, Y.; Casson, L. K.; Thomas, S. D.; Juliger, S.; Ball, M. W.; Klein, J. B.; Pierce, W. M.; Barve, S. S.; Bates, P. J. Molecular Cancer Therapeutics 2006, 5, 1790-1799.

19. Levesque, D.; Beaudoin, J. D.; Roy, S.; Perreault, J. P. Biochemical Journal 2007, 403, 129-138.

20. Phan, A. T.; Kuryavyi, V.; Gaw, H. Y.; Patel, D. J. Nature Chemical Biology 2005, 1, 167-173.

21. White, E. W.; Tanious, F.; Ismail, M. A.; Reszka, A. P.; Neidle, S.; Boykin, D. W.; Wilson, W. D. Biophys Chem 2007, 126, 140-153.

22. Chen, Q.; Kuntz, I. D.; Shafer, R. H. Proceedings of the National Academy of Sciences of the United States of America 1996, 93, 2635-2639.

23. Egholm, M.; Buchardt, O.; Christensen, L.; Behrens, C.; Freier, S. M.; Driver, D. A.; Berg, R. H.; Kim, S. K.; Norden, B.; Nielsen, P. E. Nature 1993, 365, 566-568.

24. Datta, B.; Armitage, B. A. J Am Chem Soc 2001, 123, 9612-9619.

25. Green, J. J.; Ying, L. M.; Klenerman, D.; Balasubramanian, S. J Am Chem Soc 2003, 125, 3763-3767.

26. Marin, V. L.; Armitage, B. A. Biochemistry 2006, 45, 1745-1754.

27. Marin, V. L.; Armitage, B. A. J Am Chem Soc 2005, 127, 8032-8033.

28. Datta, B.; Schmitt, C.; Armitage, B. A. J Am Chem Soc 2003, 125, 4111-4118.

29. Roy, S.; Tanious, F. A.; Wilson, W. D.; Ly, D. H.; Armitage, B. A. Biochemistry 2007, 46, 10433-10443.

30. Paul, A.; Sengupta, P.; Krishnan, Y.; Ladame, S. Chem Eur J 2008, 14, 8682-8689.

31. Rujan, I. N.; Meleney, J. C.; Bolton, P. H. Nucleic Acids Res 2005, 33, 2022-2031.

32. Ying, L. M.; Green, J. J.; Li, H. T.; Klenerman, D.; Balasubramanian, S. Proc Natl Acad Sci U S A 2003, 100, 14629-14634.

33. Phan, A.-T.; Modi, Y. S.; Patel, D. J. J Am Chem Soc 2004, 126, 8710-8716.

34. Hazel, P.; Parkinson, G. N.; Neidle, S. J Am Chem Soc 2006, 128, 5480-5487.

35. Cevec, M.; Plavec, J. Biochemistry 2005, 44, 15238-15246.

36. Hazel, P.; Huppert, J.; Balasubramanian, S.; Neidle, S. J Am Chem Soc 2004, 126, 16405-16415.

37. Risitano, A.; Fox, K. R. Nucleic Acids Res 2004, 32, 2598-2606.

38. Smirnov, I.; Shafer, R. H. Biochemistry 2000, 39, 1462-1468.

39. Smargiasso, N.; Rosu, F.; Hsia, W.; Colson, P.; Baker, E. S.; Bowers, M. T.; De Pauw, E.; Gabelica, V. J Am Chem Soc 2008, 130, 10208-10216.

40. Yamashita, M.; Fenn, J. B. J Phys Chem 1984, 88, 4451-4459.

41. Whitehouse, M.; Dreyer, R. N.; Yamashita, M.; Fenn, J. B. Anal Chem 1985, 57, 675-679.

42. Fenn, J. B.; Mann, M.; Meng, C. K.; Wong, S. F.; Whitehouse, C. M. Science 1989, 246, 64-71.

43. Ganem, B.; Li, Y.-T.; Henion, J. D. Tetrahedron Lett 1993, 34, 1445-1448.

44. Light-Wahl, K. J.; Springer, D. L.; Winger, B. E.; Edmonds, C. G.; Camp, D. G.; Thrall, B. D.; Smith, R. D. J Am Chem Soc 1993, 115, 803-804.

45. Goodlett, D. R.; Camp, D. G., II; Hardin, C. C.; Corregan, M.; Smith, R. D. Biol Mass Spectrom 1993, 22, 181-183.

46. David, W. M.; Brodbelt, J.; Kerwin, S. M.; Thomas, P. W. Anal Chem 2002, 74, 2029-2033.

47. Rosu, F.; Gabelica, V.; Houssier, C.; Colson, P.; De Pauw, E. Rapid Commun Mass Spectrom 2002, 16, 1729-1736.

48. Li, H.; Yuan, G.; Du, D. J Am Soc Mass Spectrom 2008, 19, 550-559.

49. Greig, M. J.; Gaus, H.-J.; Griffey, R. H. Rapid Commun Mass Spectrom 1996, 10, 47-50.

50. Baker, E. S.; Hong, J. W.; Gaylord, B. S.; Bazan, G. C.; Bowers, M. T. J Am Chem Soc 2006, 128, 8484-8492.

51. Modi, S.; Wani, A. H.; Krishnan, Y. Nucleic Acids Res 2006, 34, 4354-4363.

52. Delvolve, A.; Tabet, J. C.; Bregant, S.; Afonso, C.; Burlina, F.; Fournier, F. J Mass Spectrom 2006, 41, 1498-1508.

53. Hofstadler, S. A.; Griffey, R. H. Chem Rev 2001, 101, 377-390.

54. Beck, J.; Colgrave, M. L.; Ralph, S. F.; Sheil, M. M. Mass Spectrom Rev 2001, 20, 61-87.

55. Rosu, F.; De Pauw, E.; Gabelica, V. Biochimie 2008, 90, 1074-1087.

56. Gabelica, V.; Baker, E. S.; Teulade-Fichou, M.-P.; De Pauw, E.; Bowers, M. T. J Am Chem Soc 2007, 129, 895-904.

57. Mergny, J.-L.; De Cian, A.; Gheleb, A.; Sacca, B.; Lacroix, L. Nucleic Acids Res 2005, 33, 81-94.

58. Mergny, J.-L.; Gros, J.; De Cian, A.; Bourdoncle, A.; Rosu, F.; Sacca, B.; Guittat, L.; Amrane, S.; Mills, M.; Alberti, P.; Takasugi, M.; Lacroix, L. In Quadruplex Nucleic Acids, Neidle, S., Balasubramanian, S., Eds.; The Royal Soceity of Chemistry, Cambridge, 2006; Chapter 2, 31-80.

59. Gros, J.; Rosu, F.; Amrane, S.; De Cian, A.; Gabelica, V.; Lacroix, L.; Mergny, J. L. Nucleic Acids Res 2007, 35, 3064-3075.

60. Balagurumoorthy, P.; Brahmachari, S. K. J Biol Chem 1994, 269, 21 858-21 869.

61. Lu, M.; Guo, Q.; Kallenbach, N. R. Biochemistry 1992, 31, 2455-2459.

62. Rankin, S.; Reszka, A. P.; Huppert, J.; Zloh, M.; Parkinson, G. N.; Todd, A. K.; Ladame, S.; Balasubramanian, S.; Neidle, S. J Am Chem Soc 2005, 127, 10584-10589.

63. Jing, N.; Rando, R. F.; Pommier, Y.; Hogan, M. E. Biochemistry 1997, 36, 12498-12505.